



HAL
open science

Easy Acquisition and Real-Time Animation of Facial Wrinkles

Ludovic Dutreuve, Alexandre Meyer, Saïda Bouakaz

► **To cite this version:**

Ludovic Dutreuve, Alexandre Meyer, Saïda Bouakaz. Easy Acquisition and Real-Time Animation of Facial Wrinkles. *Computer Animation and Virtual Worlds*, 2011, 22 (2-3), pp.169. 10.1002/cav.395 . hal-00631255

HAL Id: hal-00631255

<https://hal.science/hal-00631255v1>

Submitted on 12 Oct 2011

HAL is a multi-disciplinary open access archive for the deposit and dissemination of scientific research documents, whether they are published or not. The documents may come from teaching and research institutions in France or abroad, or from public or private research centers.

L'archive ouverte pluridisciplinaire **HAL**, est destinée au dépôt et à la diffusion de documents scientifiques de niveau recherche, publiés ou non, émanant des établissements d'enseignement et de recherche français ou étrangers, des laboratoires publics ou privés.

Easy Acquisition and Real-Time Animation of Facial Wrinkles

Journal:	<i>Computer Animation and Virtual Worlds</i>
Manuscript ID:	CAVW-11-0033
Wiley - Manuscript type:	Special Issue Paper
Date Submitted by the Author:	07-Mar-2011
Complete List of Authors:	Dutreve, Ludovic; University of Lyon, LIRIS Meyer, Alexandre; University of Lyon, LIRIS Bouakaz, Saïda; University of Lyon, LIRIS
Keywords:	facial animation, wrinkle acquisition, fine-scale animation, RBF interpolation
Note: The following files were submitted by the author for peer review, but cannot be converted to PDF. You must view these files (e.g. movies) online.	
JCAVW2011.avi	

SCHOLARONE™
Manuscripts

1
2
3
4
5
6
7
8
9
10
11
12
13
14
15
16
17
18
19
20
21
22
23
24
25
26
27
28
29
30
31
32
33
34
35
36
37
38
39
40
41
42
43
44
45
46
47
48
49
50
51
52
53
54
55
56
57
58
59
60

Easy Acquisition and Real-Time Animation of Facial Wrinkles

Ludovic Dutreve

LIRIS - Université de Lyon

Bâtiment Nautibus (710)

43, Boulevard du 11 Novembre 1918

69622 VILLEURBANNE CEDEX

email: ludovic.dutreve@liris.cnrs.fr

Alexandre Meyer

LIRIS - Université de Lyon

Bâtiment Nautibus (710)

43, Boulevard du 11 Novembre 1918

69622 VILLEURBANNE CEDEX

email: alexandre.meyer@liris.cnrs.fr

Sada Bouakaz

LIRIS - Université de Lyon

Bâtiment Nautibus (710)

43, Boulevard du 11 Novembre 1918

69622 VILLEURBANNE CEDEX

email: sada.bouakaz@liris.cnrs.fr

Abstract

Facial animation details like wrinkles or bulges are very useful for the analysis and the interpretation of facial emotions and expressions. However, outfitting a virtual face with expression details for real-time applications is a difficult task. In this paper, we propose a mono-camera acquisition technique of facial animation details and

1
2
3
4
5
6
7
8 a technique which add a wrinkle map layer (fine-scale animation) to a skinning layer
9
10 (large-scale animation) for real-time rendering of a virtual 3D face. The acquisition is
11
12 based on ratio image computed from two pictures of a same face, with and without ex-
13
14 pression. The real-time dynamic wrinkles technique is based on a small set of reference
15
16 poses. These two methods offer an easy and low-cost way to capture facial animation
17
18 details and use it for real-time facial animation.
19
20

21
22 **Keywords:** Facial animation, wrinkle acquisition, fine-scale animation, RBF interpolation
23
24
25
26
27
28
29
30
31
32
33
34
35
36
37
38
39
40
41
42
43
44
45
46
47
48
49
50
51
52
53
54
55
56
57
58
59
60

1 Introduction

Facial animation details like wrinkles or bulges are very useful for the analysis and the interpretation of facial emotions and expressions [1]. However, outfitting a virtual face with expression details for real-time applications is a difficult task. The main reason is the difficulty to capture or synthesize wrinkle phenomena which human used to see every day, especially in a real-time context.

Since many works have been proposed for large-scale animations and deformations [2, 3], only a few of them deal with real-time animation of small-scale details on face. We denote small-scale details in an *animation* context, *i.e.* wrinkles and bulges appearing while muscles contractions, instead of the micro-structures of the skin independent to facial expressions. An interesting approach was proposed by Oat [4], it consists on blending wrinkle maps to render animated details on a human face. This technique provides good results at an interactive time by using common bump-mapping technique for the rendering. However, it requires manual tuning of blending coefficients, leading to manual efforts for each new animation, and requires wrinkle maps which may be difficult to create.

Capturing these facial animation details is still a challenging issue. On one hand, current capture methods focus on capturing the whole 3D geometry of a face with heavy active system based on lasers, structured lights or gradient-based illumination, with multiple cameras [5, 6, 7]. Even if recent researches propose passive systems [8, 9], stereo aspect is still the minimum, with often six or more high resolution cameras. On the other hand, many appli-

1
2
3
4
5
6
7
8 cations want to apply captured motions to other faces than the one filmed. Thus, they do not
9
10 need 3D high resolution meshes of the actor from which desired features are hard to extract
11
12 and to transfer.
13

14
15 In this paper, we propose two techniques to both capture details and apply them on a
16
17 real-time facial animation. To avoid complex motion capture system, we propose an easy
18
19 and low-cost technique to capture facial details. On several frontal photos of different facial
20
21 expressions, we capture corresponding normal maps with a few manual effort of landmark-
22
23 ing on pictures. By considering only frontal single-camera views, we address the problem of
24
25 normal reconstruction using the shading information in an inverse problem, where classical
26
27 facial capture approaches use stereo. Our dynamic wrinkle technique consists on adding a
28
29 wrinkle map layer to a skinning layer. The skinning layer is a common bone-based large-
30
31 scale animation technique on which we add the fine-scale details thanks to a local-area based
32
33 wrinkle map layer. In order to apply wrinkle map, we use a small set of reference poses.
34
35 A reference pose is a pair of a large-scale deformation (a skeleton pose) and its associated
36
37 small-scale details (a wrinkle map). During the animation, the current skeleton pose is com-
38
39 pared with the reference poses and wrinkle maps coefficients are automatically computed
40
41 with the use a non-linear function. Notice that comparison is done at a bone level resulting
42
43 in local blends and independence between areas of the face.
44
45
46
47
48
49
50
51
52
53
54
55
56
57
58
59
60

2 Related Work

Since our approach is based on single camera for the normal maps acquisition, we focus on single image shape reconstruction, and specially on inverse shading approaches which have to be classified in the class of Shape from Shading (SfS) problems. The SfS problem has been widely studied in the computer vision area [10]. It is known as difficult because of its ill-posedness [11]. Consequently, few approaches have been tried on real photographs [12]. By considering the normal-map reconstruction instead of the 3D shape we relax a bit the difficulty of the problem [13]. Moreover, normal maps are well suited to real-time rendering and to our wrinkles-synthesis-from-example method. Wu *et al.* propose an interesting interactive normal reconstruction from a single image [13]. By aiming at reconstructing only local features such as wrinkles, we can limit the phase of user interaction which is mainly dedicated to give global information. Considering photo of face gives an a priori on the shape form which helps to solve the ill-posedness aspect and allows to reconstruct the large scale aspect of a face [14]. To our knowledge, state of the art on SfS (understanding mono-camera) does not show convincing results on skin wrinkles acquisition. Thus, they are often procedurally synthesized [15].

While some techniques were proposed to generate wrinkles on arbitrary surface [16, 17], few approaches focused on real-time facial applications. Larboulette *et al.* proposed a technique to simulate dynamic wrinkles [18]. The user defines wrinkling areas by drawing a perpendicular segment of wrinkles (wrinkling area), following by the choice of a 2D discrete

1
2
3
4
5
6
7 control curve (wrinkle template). The control curve conserves its length while the mesh
8 deformation, generating amplitude variations. Wrinkles are obtained by mesh subdivision
9 and displacement along the wrinkle curve. Many methods need a high resolution mesh or a
10 *on-the-fly* mesh subdivision scheme to generate or animate wrinkles [19, 20]. Due to real-
11 time constraints and the resource sharing, these techniques may be difficult to use in an
12 efficient way. GPU computing allows to render efficiently fine details by using bump maps
13 for interactive rendering. Oat presented in [4] a GPU technique to easily blend wrinkle maps
14 applied to a mesh. Maps are subdivided in regions, for each region, coefficients allow to
15 blend the wrinkle maps. This technique requires few computational and storage costs, three
16 normal maps are used for a neutral, a stretched and a compressed expressions. Furthermore
17 it is easily implemented and added to an existing animation framework. The main drawback
18 of this method is that it requires manual tuning of the wrinkle maps coefficients for each
19 region. Similarly, De Melo *et al.* synchronize a normal map with a pseudo-muscular model
20 to avoid manual coefficient tuning [21]. Normal maps are obtained by a manual image
21 manipulation step. They directly use luminance information on a single photography and
22 manually fit details to the character's texture. Our details extraction approach is more formal
23 and requires less manual intervention. Our animated details method aims at providing a
24 real-time dynamic wrinkling system for skinned face which generates automatically wrinkle
25 maps coefficients and does not require a mask map.
26
27
28
29
30
31
32
33
34
35
36
37
38
39
40
41
42
43
44
45
46
47
48
49
50
51
52
53
54
55
56
57
58
59
60

3 Acquisition of the skin details normal maps

In this section, we detail how we capture the skin details normal maps of several facial expressions. Since we do not need to capture the entire geometry of the face, our approach uses the illumination variation between two pictures of a same face with different expressions. Let \mathcal{I} be the image of the neutral pose, and \mathcal{I}' the image of the expression pose where the details we want to extract are. We seek to compute the normal map which will be applied during the real-time facial animation to produce details.

3.1 Normal map generation

The first step of our method consists of computing the ratio image to extract light variation [22]. In order to work on pixel at correct positions, we start to deform \mathcal{I}' into \mathcal{I}'_d to fit \mathcal{I} . This allows us to obtain a mapping between each pixel, and so, to know the difference of illumination at each point of the face surface. The deformed image \mathcal{I}'_d is obtained by using a Radial Basis Functions (RBF) scattered data interpolation [23] between two sets of landmarks manually picked on the two images \mathcal{I} and \mathcal{I}' . The ratio image \mathcal{R} is computed by dividing \mathcal{I} to \mathcal{I}'_d :

$$\mathcal{R} = \frac{\mathcal{I}'_d}{\mathcal{I}} \quad (1)$$

Then, we perform a blurring filter to \mathcal{R} to reduce acquisition noise. To avoid artefacts due to eventual registration errors, we give the possibility to define regions of interest with

a simple painting tool. Furthermore, these masks help to avoid defining a large number of landmarks to obtain a perfect mapping, even in the areas that the user does not need to extract features. Figure 1 shows an example of pictures of different expressions with the associated ratio image.

Let C_d the intrinsic color of the skin, C_l the color of the light, $\vec{N} = (N_x, N_y, N_z)^t$ (resp. $\vec{N}' = (N'_x, N'_y, N'_z)^t$) the normal at the surface of the skin of the neutral image (resp. the interpolated expression image¹), and \vec{L} the light-direction vector. If we assume that skin is a diffuse surface, under the Lambertian model, $I = C_d \times C_l \times \vec{N} \cdot \vec{L}$ and $I'_d = C_d \times C_l \times \vec{N}' \cdot \vec{L}$. We will retrieve \vec{N}' in two step: the normal tilt N'_z and the normal orientation (\vec{N}'_x, \vec{N}'_y) . The Formula 1 gives:

$$\mathcal{R} = \frac{I'_d}{I} = \frac{C_d \times C_l \times \vec{N}' \cdot \vec{L}}{C_d \times C_l \times \vec{N} \cdot \vec{L}} = \frac{\vec{N}' \cdot \vec{L}}{\vec{N} \cdot \vec{L}} \quad (2)$$

By using the flash light of the camera, we can approximate the light direction to $\vec{L} = (0, 0, -1)$, given $\mathcal{R} = N'_z/N_z$. We make the approximation that regions of interest are locally plane at the neutral pose. By default, we assume that these planes are parallel to the camera plane, resulting in $N_z = 1$, but the user can define different values for N_z if considered necessary, to refine the result.

Equation 2 shows that the ratio image intensity is dependant to the orientation of the surface. More \mathcal{R} is dark, more N'_z is small and more the wrinkles are deep. Notice that this use of the ratio image avoids the painful problem of finding the intrinsic color from a photo.

¹Notice that we work into the tangent coordinate system of the neutral image.

1
2
3
4
5
6
7 We should now compute the normal orientation (\vec{N}_x, \vec{N}_y) for a given pixel of the wrinkles
8
9 at each pixel. For this, N'_z is not enough. We assume that the gradient of the image ratio is
10
11 a good approximation of the normal orientation, which is mainly similar to the assumption
12
13 done in [24, 25]. Let G_x and G_y be the 2D normalized gradient of \mathcal{R} for the two axes \vec{x}
14
15 and \vec{y} . We want to find N'_x and N'_y such that $N_x'^2 + N_y'^2 + N_z'^2 = 1$, and $N'_x = \alpha G_x$ and
16
17
18
19
20
21
22
23
24
25
26
27
28
29
30
31
32
33
34
35
36
37
38
39
40
41
42
43
44
45
46
47
48
49
50
51
52
53
54
55
56
57
58
59
60
 $N'_y = \alpha G_y$ with α a normalization coefficient. We obtain the formulae:

$$\begin{aligned} N'_x &= G_x \times \sqrt{1 - N_z'^2} \\ N'_y &= G_y \times \sqrt{1 - N_z'^2} \end{aligned} \quad (3)$$

We then convert \vec{N}' into a normal map norm. Figure 1 illustrates a normal map obtained with a ratio image.

3.2 3D character adaptation

The last step we perform for details acquisition is the interpolation between the capture space to character texture space. It aims at ranging the computed normal map to the character. We use the same method as for the interpolation between the neutral and the expression images, two sets of landmarks are manually defined on both normal map and character's texture map, and a RBF based interpolation deformed the first to the second (see Figure 2).

4 Real-Time Fine Details Animation

Our goal is to add a wrinkle map layer (fine-scale animation layer) to a bone-based facial animation (large-scale animation). We use the wrinkles data captured at the acquisition step to generate on the fly visual dynamic fine details such as wrinkles or bulges on the face surface. We explain in this section how we use a small set of reference poses in real-time and at arbitrary poses.

4.1 Reference Poses

A reference pose is a pair of a large-scale deformation (a skeleton pose) and its associated small-scale details (stored in the form of a normal map we call wrinkle map). To create a reference pose, we deform the facial skeleton to obtain the expression on which we want the wrinkles appear. This expression should be strongly pronounced to provide better results. Then, we associate to the pose a wrinkle map extracted in the acquisition step. Since influences work with bones or group of bones, it is possible to define a pose where wrinkles appear in various areas of the face. Having details in different areas will not cause that all of these details appear at the same time at an arbitrary frame. For example, details around the mouth would appear independently with forehead details, even if they are described in a same reference pose.

4.2 Pose Evaluation

While runtime, the first step is to compute the influence of each reference pose on each bone. This consists in finding how the bone position at an arbitrary frame looks like its position at the reference poses². Computing these influences at the bone level instead of a full pose level allows to determine regions of interest. This offers the possibility to apply different reference poses at a same time. Resulting in the need of less reference poses (actually, only 2 may be sufficient for face: a stretched and a compressed expression).

We define the influence α_{jfk} of the pose Π_k for the bone P_j at the position \vec{P}_{jf} for the arbitrary pose Π_f by the following equation:

$$\alpha_{jfk} = \min \left(1, \max \left(0, \frac{\vec{AB} \cdot \vec{AC}}{\|\vec{AC}\|} \right) \right) \quad (4)$$

where $\vec{AB} = (\vec{P}_{jf} - \vec{P}_{j0})$, $\vec{AC} = (\vec{P}_{jk} - \vec{P}_{j0})$, \cdot denotes the dot product and $\|\dots\|$ denotes the Euclidean distance. α_{jfk} is the size of the segment between the orthogonal projection of \vec{P}_{jf} on the segment $[\vec{P}_{jk}, \vec{P}_{j0}]$ normalized by the size of the segment $[\vec{P}_{jk}, \vec{P}_{j0}]$.

4.3 Bones Masks

Once we know the reference poses influences for each bone, we could use them for the per-pixel lighting. The main idea is to use skinning weights to compute the influence of

²Notice that we deal with bones positions in the head root bone coordinates system, so we could assume that head rigid transformation will not cause problems while pose evaluation.

reference poses for each vertex, and by the interpolation done during the rasterization phase, for each fragment (Fig. 3). Since wrinkles and expressive details are greatly related to the face deformations, we can deduce that these details are related with bones transformations too. So we associate bones influence with reference poses influences. A mesh vertex v_i with a skinning weight of w_{ij} with the bone P_i is influenced by the reference pose Π_k at the arbitrary pose Π_f such as:

$$\beta_{ifk} = \sum_{i=1}^n \lambda_{ij} \times \theta(\alpha_{jfk}) \quad (5)$$

with

- $\lambda_{ij} = 1$ if $w_{ij} > 0$ and $\lambda_{ij} = 0$ else;
- $\theta(x)$ the modulation function described in the next section.

4.4 Modulation function

Wrinkles do not appear on face linearly according to bones displacements. Indeed, two bones moving from the neutral position to the compressed one will create wrinkles more intensively at this end of the movement than at the beginning. For this purpose, we introduce during the synthesis phase a non-linear function θ such as $\theta : [0, 1] \rightarrow [0, 1]$ which rules this phenomena by modifying the distance used during the normal map blending. To propose a function based on real wrinkles apparition, we run our normal map acquisition algorithm on each frame of a video sequence where a face start from a neutral pose to an expressive

1
2
3
4
5
6
7
8 one. It provides for each pixel and for a given bones configuration, a vector of normal map
9 displacement. The length of this vector indicates the intensity of the wrinkles. Since the
10 wrinkle synthesis is done on the GPU, it would have been inefficient to store for each pixel
11 a set of discrete values for each bones configurations. We preferred fit an analytic curve:
12
13
14
15
16

$$\theta(x) = \frac{\cos(\pi(1+x)) + 1}{2} \quad (6)$$

17
18
19
20
21

22 Figure 4 shows the segment curve we capture and the curve we propose. The cosine function
23 seems to be an interesting base if we apply to it a translation and a normalization to check our
24 constraints. We try to depict a smooth and progressive acceleration of wrinkles amplitude.
25
26
27
28
29 We give priority to highest percentage of deformation, when wrinkles are deepest, whereas
30 the distance between the two curves, which seems high at the begin of the deformation,
31 produces only a weak visual impact. Notice that user can define a new function and/or
32 capture his own data to better fit his needs if necessary.
33
34
35
36
37
38
39
40

41 **4.5 Details Blending**

42
43

44 The final step of our method is to apply wrinkle maps to our mesh by using coefficients
45 $\theta(\beta_{i,k})$ computed at the previous step. Since normal maps only contain deformations asso-
46 ciated with the expression, we should apply a finest blending to avoid loss of static details
47 located on the neutral normal map (*i.e.* details such as pores, scars and other static fine
48 details). For example, with a simple averaging, a fragment influenced by 100 percents of a
49 wrinkle map will be drawn without using the neutral map, resulting in the fact that details
50
51
52
53
54
55
56
57
58
59
60

of the neutral map will not appear. Let \vec{n}_f the final normal, \vec{n}^i the ρ normals provided by the wrinkle maps, their coefficients w^i and \vec{n} the normal provided by the default normal map, we first compute weighted normals η^i of the wrinkle maps and then compute the final normal:

$$\eta^i = (0, 0, 1)^t + w^i \times (n^i - (0, 0, 1)^t) \quad (7)$$

$$\vec{w}_f = \begin{pmatrix} n_x + \sum_{i=1}^{\rho} \rho \eta_x^i \\ n_y + \sum_{i=1}^{\rho} \eta_y^i \\ n_z \times \prod_{i=1}^{\rho} \eta_z^i \end{pmatrix} \quad (8)$$

The addition of the two first coordinates makes a simple averaging between the direction of the two normals, given the desired direction. The z components are multiplied, this leads to increase details obtained from the two normals. More z is small, and more the surface will be bumpy, multiplication allows to add the neutral surface variation to the wrinkled surface.

5 Results and Discussion

Our acquisition technique provides good results with a few effort and material. Despite the lighting model approximation, which does not take into account the specular reflection of the skin, we obtain very interesting visual results. Our method provides an alternative to

1
2
3
4
5
6
7
8 others facial motion captures systems if the goal is to obtain only animation fine-scale details
9
10 and not the full geometry of the face. Figure 5 shows an example of use of a captured normal
11
12 map by our monocular acquisition technique.
13

14
15 Our 3D test models *Proog*³ is about 10000 triangles. The faces is rigged with 21 bones.
16
17 Animation runs at more than 100 fps on a common personal computer with an Athlon
18
19 64 3800+ CPU, 3Go RAM and a NVidia Geforce GTX 275 GPU. The Figure 6 shows the
20
21 neutral and the two reference poses used for demonstration. The Figure 7 shows the 6 basis
22
23 expressions of *Proog* with and without our dynamic wrinkles and the Figure 5 shows the
24
25 possibility to apply dynamic details on different area of the face even if details are given on
26
27 a same wrinkle map.
28
29
30

31
32 Large scale skinning-based deformation are not modified. The addition of our method
33
34 to an existing implementation is easy. No additional rendering pass is required. Our choice
35
36 to use skinning weights as bones masks offers many advantages. They allow us to relate
37
38 large scale and small scale deformations, and so, we do not need additional mask textures.
39
40 They ensure that vertices influenced by reference poses are vertices which are displaced
41
42 accordingly with bones too.
43
44
45

46
47 Although our technique easily provides wrinkles on facial animation, several steps are
48
49 important to obtain good results. First, a good rigging is primary since we directly use
50
51 skinning weights as bones masks, and so, it defines how each vertex will be influenced by the
52
53

54 ³©Copyright 2006, Blender Foundation / Netherlands

1
2
3
4
5
6
7 different reference poses. Second, the reference poses should consist on an orthogonal set of
8 skeleton poses as much as possible, to avoid an over fitting. Notice that blending reference
9 poses in a same area is possible but it becomes a problem if similar bones displacements lead
10 to different fine-details. Finally, detail maps quality greatly influences the visual results.
11 Problems occur when capturing faces with beard where mouth details can not be obtain
12 because of the incoherence in the ratio computation. Our approach is more suited to soft
13 skin subjects.
14
15
16
17
18
19
20
21
22
23
24
25
26

27 **6 Conclusion**

28
29
30
31 We have presented two techniques. The first aims at capturing facial animation details from
32 two pictures of a same face with and without expression. It requires few manual work and
33 does not need specific material. A simple camera with its flash light was used. The second
34 is a technique which use reference poses to generate non-linearly in real-time wrinkles and
35 fine-details appearing with an arbitrary skinned face animation. In addition to providing
36 interesting visual results, the requirements that we considered necessary and/or important
37 have been met. Our dynamic animation wrinkles runs in real-time, the use of per-pixel
38 lighting allows us to dispense with high-resolution meshes or costly subdivision techniques.
39 Furthermore, it is based on widely-used techniques such as skinning and bump mapping. Its
40 implementation does not present technical difficulties and does not modify usual animation
41 and rendering pipeline. In futur works, it may be interesting to consider specular reflection
42
43
44
45
46
47
48
49
50
51
52
53
54
55
56
57
58
59
60

1
2
3
4
5
6
7
8 of the skin in our acquisition step. We will also try to improve our image-based details
9
10 extraction to a video-based one, allowing to apply wrinkles in real-time from a captured
11
12 face. Regarding the 3D aspect, last advances in graphics hardware provide local tessellation
13
14 ability, it should be easy to adapt our bump-map method to a local mesh refinement with
15
16 very similar input textures.
17
18
19
20
21

22 **References**

- 23
24
25
26 [1] M. Courgeon, S. Buisine, and J.-C. Martin. Impact of expressive wrinkles on percep-
27
28 tion of a virtual character's facial expressions of emotions. In *IVA*, 2009.
29
30
31
32 [2] N. Ersotelos and F. Dong. Building highly realistic facial modeling and animation: a
33
34 survey. *Vis. Comput.*, 2007.
35
36
37
38 [3] J. Gain and D. Bechmann. A survey of spatial deformation from a user-centered per-
39
40 spective. *ACM Trans. Graph.*, 2008.
41
42
43
44 [4] C. Oat. Animated wrinkle maps. In *ACM SIGGRAPH 2007 courses*, 2007.
45
46
47
48 [5] T. Weise, B. Leibe, and L. Van Gool. Fast 3d scanning with automatic motion com-
49
50 pensation. In *CVPR*, 2007.
51
52
53 [6] O. Alexander, M. Rogers, W. Lambeth, M. Chiang, and P. Debevec. The digital emily
54
55 project: photoreal facial modeling and animation. In *ACM SIGGRAPH Courses*, 2009.
56
57
58
59
60

- 1
2
3
4
5
6
7
8 [7] C. A. Wilson, A. Ghosh, P. Peers, J.-Y. Chiang, J. Busch, and P. Debevec. Tempo-
9
10 ral upsampling of performance geometry using photometric alignment. *ACM Trans.*
11
12 *Graph.*, 2010.
- 13
14
15
16 [8] T. Beeler, B. Bickel, P. Beardsley, B. Sumner, and M. Gross. High-quality single-shot
17
18 capture of facial geometry. In *ACM Trans. Graph.*, 2010.
- 19
20
21
22 [9] D. Bradley, W. Heidrich, T. Popa, and A. Sheffer. High resolution passive facial per-
23
24 formance capture. In *ACM Trans. Graph.*, 2010.
- 25
26
27
28 [10] J.-D. Durou, M. Falcone, and M. Sagona. Numerical methods for shape-from-shading:
29
30 A new survey with benchmarks. *Comput. Vis. Image Underst.*, 2008.
- 31
32
33
34 [11] E. Prados and O. Faugeras. Shape from shading: a well-posed problem ? In *CVPR*,
35
36 2005.
- 37
38
39 [12] O. Vogel, L. Valgaerts, M. Breuß, and J. Weickert. Making shape from shading work
40
41 for real-world images. In *DAGM*, 2009.
- 42
43
44
45 [13] Tai-Pang Wu, Jian Sun, Chi-Keung Tang, and Heung-Yeung Shum. Interactive normal
46
47 reconstruction from a single image. *ACM Trans. Graph.*, 2008.
- 48
49
50
51 [14] W. A. Smith and E. R. Hancock. Facial shape-from-shading and recognition using
52
53 principal geodesic analysis and robust statistics. *IJCV*, 2008.
- 54
55
56
57
58
59
60

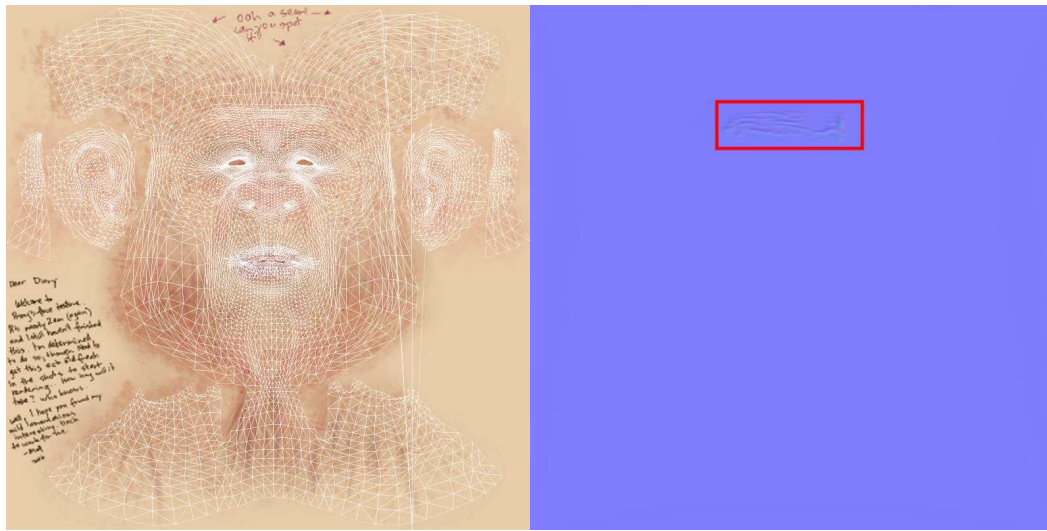
- 1
2
3
4
5
6
7 [15] B. Bickel, M. Botsch, R. Angst, W. Matusik, M. Otaduy, H. Pfister, and M. Gross.
8 Multi-scale capture of facial geometry and motion. In *ACM Trans. Graph.*, 2007.
9
10
11
12 [16] Y. Bando, T. Kuratate, and T. Nishita. A simple method for modeling wrinkles on
13 human skin. In *PG*, 2002.
14
15
16
17 [17] H. Wang, F. Hecht, R. Ramamoorthi, and J. O'Brien. Example-based wrinkle synthesis
18 for clothing animation. *ACM Trans. Graph.*, 2010.
19
20
21
22 [18] C. Larboulette and M.-P. Cani. Real-time dynamic wrinkles. In *Comp. Graph. Int.*,
23 2004.
24
25
26
27 [19] Y.-S. Lo, I.-C. Lin, W.-X. Zhang, W.-C. Tai, and S.-J. Chiou. Capturing facial details
28 by space-time shape-from-shading. In *Comp. Graph. Int.*, 2008.
29
30
31
32 [20] K. Na and M. Jung. Hierarchical retargetting of fine facial motions. In *Comp. Graph.*
33 *Forum*, 2004.
34
35
36
37 [21] C. de Melo and J. Gratch. Expression of emotions using wrinkles, blushing, sweating
38 and tears. In *IVA*, 2009.
39
40
41
42 [22] Z. Liu, Y. Shan, and Z. Zhang. Expressive expression mapping with ratio images. In
43 *ACM Trans. Graph.*, 2001.
44
45
46
47 [23] A. M. Siddiqui, A. Masood, and M. Saleem. A locally constrained radial basis function
48 for registration and warping of images. *Pattern Recogn. Lett.*, 2009.
49
50
51
52
53
54
55
56
57
58
59
60

- 1
2
3
4
5
6
7
8 [24] R. J. Woodham. Photometric method for determining surface orientation from multiple
9
10 images. *Optical Engineering*, 1980.
11
12
13 [25] A. Robles-Kelly and E. R. Hancock. Shape-from-shading using the heat equation.
14
15 *IEEE Trans. on Image Processing*, 2007.
16
17
18
19
20
21
22
23
24
25
26
27
28
29
30
31
32
33
34
35
36
37
38
39
40
41
42
43
44
45
46
47
48
49
50
51
52
53
54
55
56
57
58
59
60



(a) neutral expression (b) expression with details (c) interpolated expression (d) mask (e) ratio image (f) normal map

Figure 1: Ratio image computation using two pictures of a same face with two expressions and a mask to specify where details we want to capture are. The last image is the normal map obtained from the ratio image and its gradients.



(a) texture map

(b) new normal map

Figure 2: Interpolation of the extracted normal map (Fig. 1f) to fit the 3D character texture space (a).

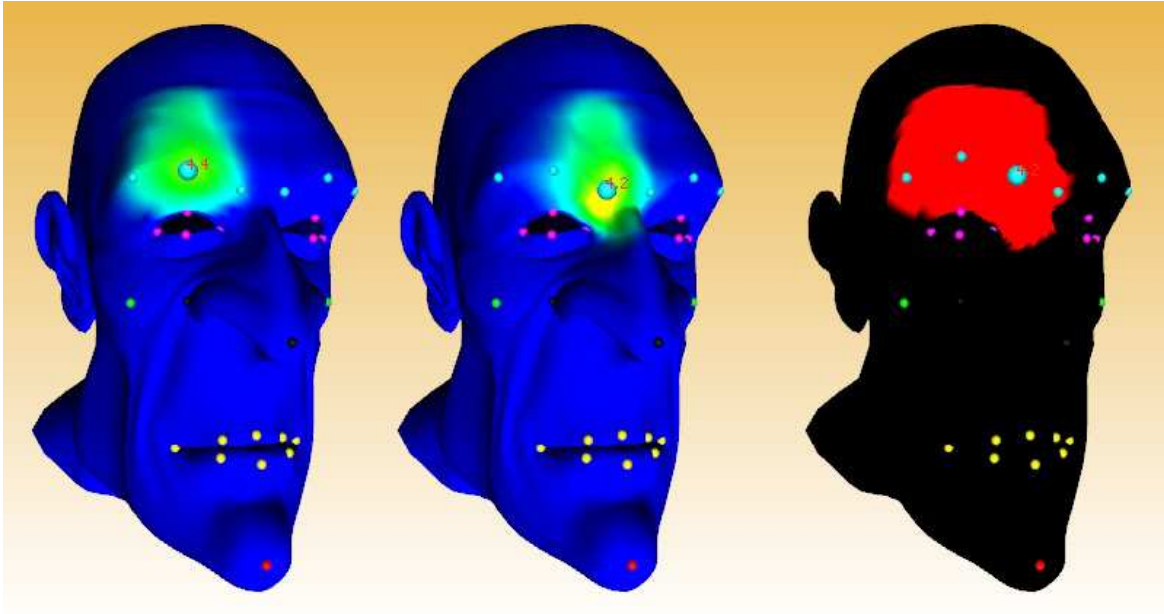


Figure 3: The two left images show the skinning influences of two right eyebrow bones. The third image shows the influence of a reference pose for each vertex attached to these bones.

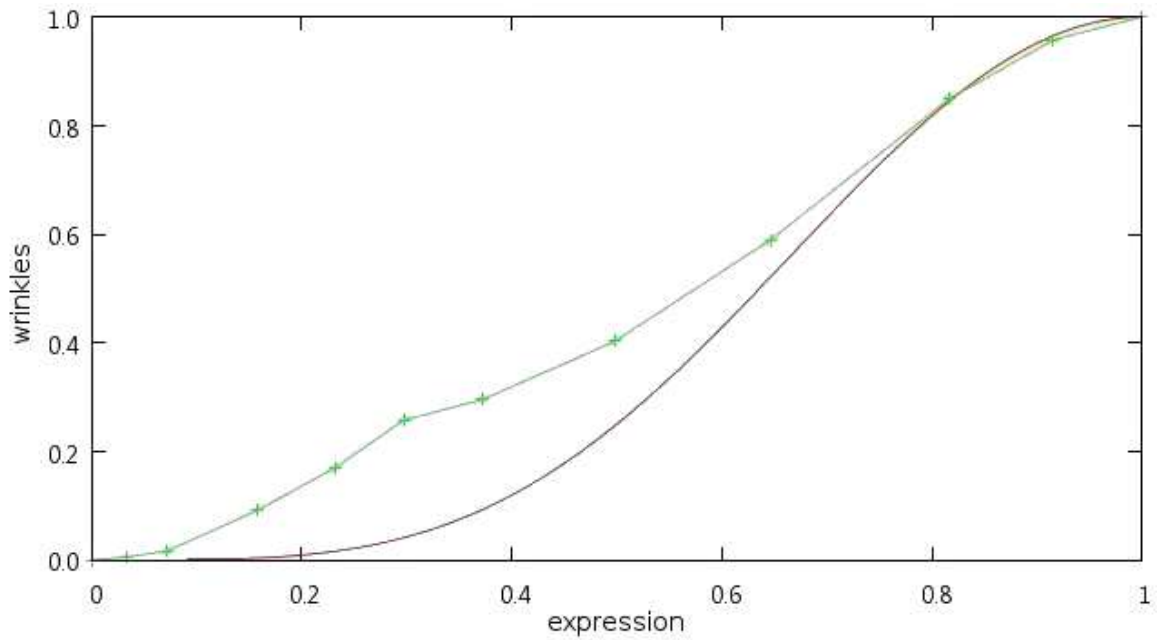


Figure 4: In green: the capture curve, in red: the function we propose for wrinkle appearance by the reference pose ratio.



Figure 5: Example of acquired normal map applied on our target character.

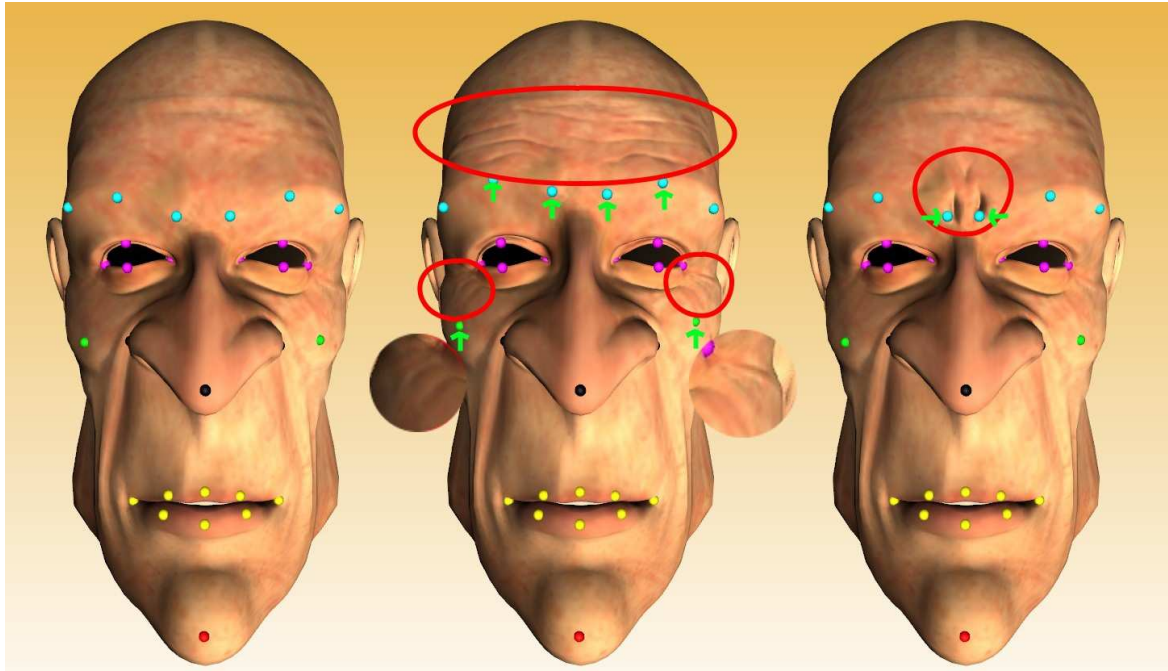


Figure 6: The neutral and the 2 reference poses.

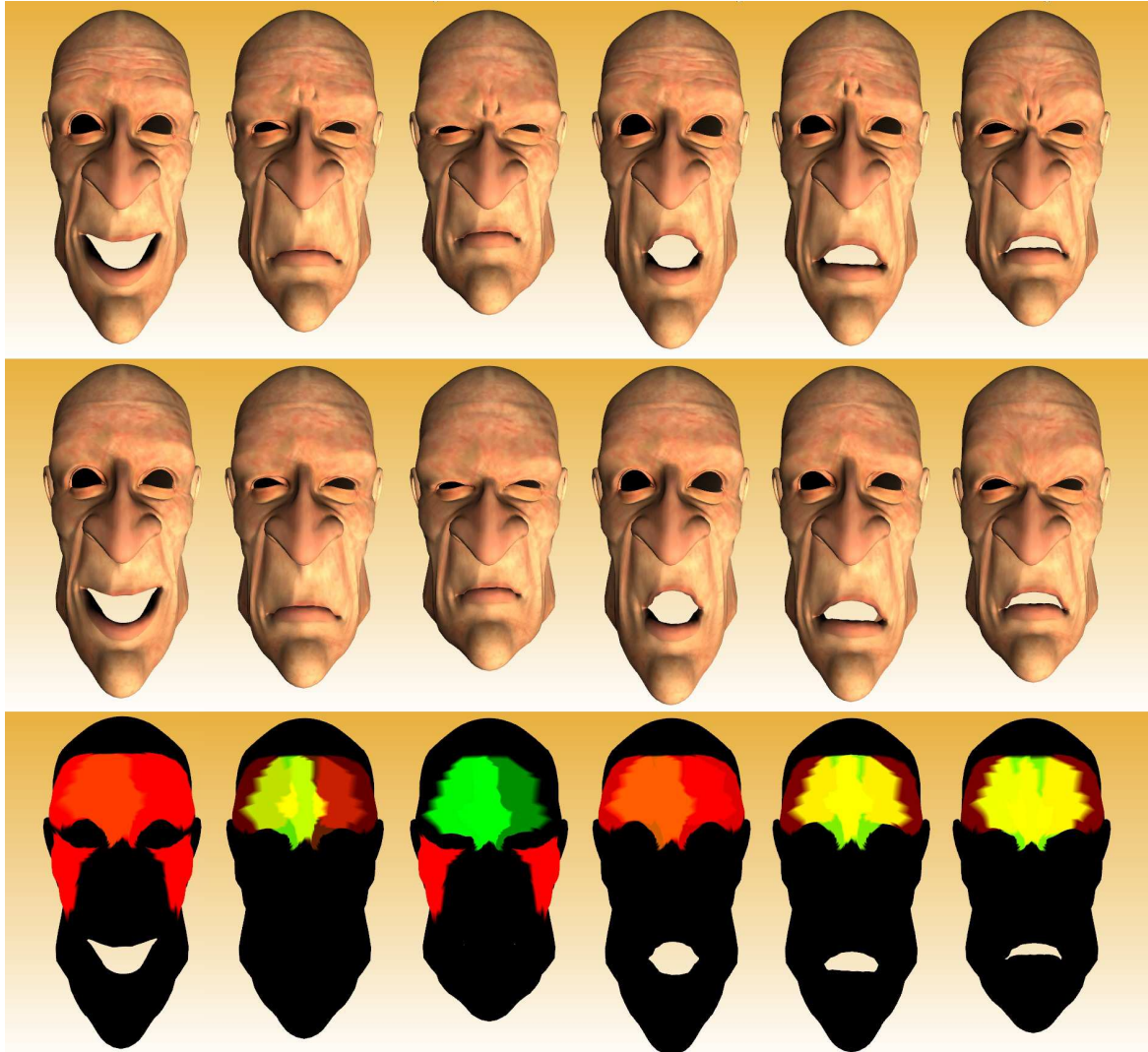


Figure 7: The first row shows the 6 basis expressions (joy, sad, disgust, surprise, fear, angry) of our character with captured dynamic wrinkles. The second row shows the same expressions without dynamic wrinkles. The last row shows the reference poses influences on the mesh (red for the first reference pose, and green for the second).